uc3m | Universidad Carlos III de Madrid

e-Archivo

This is a postprint version of the following published document:

Martinez-Cisneros, C., Antonelli, C., Levenfeld, B., Varez, A., Pérez-Flores, J., Santos-Méndez, A., Kuhn, A. & Sanchez, J. Y. (2021). Non-woven polyaramid porous membranes as separators for Li-ion batteries? *Electrochimica Acta, 390*, 138835.

DOI: 10.1016/j.electacta.2021.138835

© 2021 Elsevier Ltd. All rights reserved.

This work is licensed under a Creative Commons Attribution-NonCommercial-NoDerivatives 4.0 International License.

Non-woven polyaramid porous membranes as separators for Li-ion batteries?

C. Martinez-Cisneros[1*], C. Antonelli[2], B. Levenfeld[1], A. Varez[1], J. C. Pérez-Flores[3], A. Santos Méndez[3,5], A. Kuhn[3], J-Y. Sanchez[1,4*]

[1] Materials Science and Engineering Department, Universidad Carlos III de Madrid, Spain.

[2] Institut Européen des membranes (IEM), UMR-5635, Université de Montpellier, ENSCM, CNRS, Place Eugène Bataillon, 34095 Montpellier cedex 5, France

[3] Departamento de Química y Bioquímica, Facultad de Farmacia, Universidad CEU San Pablo, Madrid, Spain

[4] University Grenoble Alpes, LEPMI, 38000 Grenoble, France.

[5] Mindcaps Smart Supercapacitors S.L. 28020 Madrid, Spain

Corresponding authors: *jeasanch@ing.uc3m.es, *cymartin@ing.uc3m.es

Abstract

Macroporous separators play a crucial role regarding safety in current Li-ion batteries. Most separators used in battery applications are based on polyolefin and present shrinkage and a decrease in mechanical properties when used at high temperatures, both detrimental in the battery performance. In search of more suitable alternatives that render to more stable and safer batteries, in this work, non-woven separators based on polyacrylonitrile blended with cellulose and para-aramid fibers are systematically investigated. This study has been carried out in terms of

microstructure, mechanical properties, ionic conductivity and thermal and electrochemical stability (using $Li_4Ti_5O_{12}/LiCoO_2$ full cells with a nominal potential of ≈2.5 V). Although conductivity values of separators are somewhat modest, the electrochemical performance developed when used in a $Li_4Ti_5O_{12}/LiCoO_2$ cells are, at moderate C rates, comparable to commercial Celgard©2400 separator. At high C rates, in particular at 2C, DwG40 exhibits much higher capacities than the whole of the separators, including Celgard®2400. This study responds to the continuous need reflected not only by the scientific community but also by the industrial one when new materials for electrolytes and electrodes should be tested, since there is a lack of reports characterizing such elements in the literature.

Keywords: non-woven separator; macroporous polymer membrane; microporous polymer membrane; Li-ion battery.

1. Introduction

Materials used as macroporous[1] separators in batteries based on liquid electrolytes are often appointed as inactive, since they do not participate directly in any electrochemical reaction. Nevertheless, they are a strategic, crucial and costly component of lithium-ion batteries [1–4]. Their role consists on separating the electrodes, avoiding any physical contact between them, in order to prevent a short circuit and to ensure ionic transport, with a minimum internal resistance, to reach an optimized ionic conductance. In this way, the separators properties influence directly the cell performances and its lifetime just as its reliability, safety and cost. With the aim to fulfil all these expectations, separators should meet many criteria in terms of electrochemical and thermal stability, mechanical properties, wettability, permeability and dimensional and morphological stability [1–6]. Each criterion has its own requirements and sometimes some of them may be antagonists. For instance, separators should be as thin as possible and sufficiently

[1] Microporous is extensively used but regarding the average pore size they should be named macroporous following the IUPAC rules. In the text we will use macroporous.

porous to favor ionic conductivity without leading to loss in mechanical properties, which would be detrimental in terms of safety. Therefore, it is necessary to identify the dominant criterion and optimise the balance with the other one towards achieving a high performance separator. Nowadays, polyolefin-based separators dominate the market and are mainly produced by five manufacturers [4]. Most of the time, they consist of a macroporous separator, whose configuration could be a single or a multilayer system, providing in both cases a relatively good electrochemical stability, mechanical properties (high strength) and ionic conductivity. Nevertheless, these non-polar separators present important drawbacks, including low wettability regarding polar liquid electrolytes, poor electrolyte retention and, above all, limited thermomechanical stability. Even though the presence of a shutdown layer contributes to limit drawbacks in terms of safety, polyolefin-based separators generally exhibit a significant shrinkage phenomenon between 120°C and 140°C, or even at lower temperatures, at longer operating time. This may result in internal short circuit and, therefore, thermal runaway [7]. In this sense, thermomechanical stability of separators is one of the key issues in order not only to achieve high-safety, large-scale and high performance lithium-ion batteries but also to meet the demands of new applications, in particular, the automotive industry, regarding the development of electrical and hybrid vehicles [8]. Following a conservative strategy, polypropylene coating with aluminum phosphate partially solve the inherent problems of polyolefin-based separators [9]. More recently, porous PVDF-based membranes are an appealing alternative as they allow porosity control [10] and improve thermal stability [11].

Trying to provide safer conditions, non-woven separators have been proposed as an alternative, since they generally present an improved thermal stability. Non-woven separators, mainly based on natural or polyimide fibers, are characterized by a high porosity, a good electrolyte affinity (wettability) and enhanced mechanical properties. Moreover, they also provide efficient cycling performance as well as ionic conductivity. Nevertheless, their application is currently limited to alkaline batteries, since their use in lithium-ion batteries is restricted given their “open” structure [5]. Indeed, their high porosity is often formed by large non-uniform pore sizes, which facilitate

the formation of dendrites and the penetration of particles, e.g. carbon and/or active material possibly released by the composite, leading to internal short circuit or current leakage. Hence, a simple approach consists on increasing the thickness of the separator or using it as a supported layer. In order to expand their application to Li-ion batteries, non-woven separators have been recently proposed for their commercialization. In this sense, Dreamweaver Intl. has proposed two ranges of non-woven separators, among others, named Silver and Gold, which address lithium-ion batteries for high power applications. These separators, manufactured by wet-laid processing, consist of a combination of microfibers and cellulose nanofibers, providing a good wettability regarding organic polar solvents. Silver separators are based on polyacrylonitrile nanofibers blended with cellulose; whereas Gold separators are made from Twaron® para-aramid microfibers. Both are highly porous (Table 1) and provide good thermal stability [12], exhibiting 8% and 2% of shrinkage at 300°C for Silver and Gold separators, respectively. Results of a series of tests (nail penetration test, hot box tests and hard short and overcharge tests) performed on $LiFePO_4$ /graphite pouch cells of 2700 mAh capacity have been reported and compared with different commercial separators with shutdown function [13]. According to these results, these separators present improved thermal stability and only suffer of primary mechanical damages; whereas other commercial separators show shrinkage and cracking phenomena. In a recent study, mechanical properties of 40 μm thick Gold separators have been evaluated in stress conditions over a range of strain rates, showing an isotropic behavior [14]. These kinds of non-woven separators have been already used to evaluate the safety performances of new electrolytes [15], but without any consideration on the performance of the separators [1]. In this way, the aim of this work is to evaluate the main characteristics and properties (microstructural, thermal, mechanical, conductivity, etc.) of specific Dreamweaver separators. Physical and electrochemical results of this study state on their abilities to be used in lithium-ion batteries, especially for their future use in an extended temperature range for high temperature applications. Therefore, a systematic characterization of the separators has been performed in terms of microstructure, mechanical properties, ionic conductivity and thermal and electrochemical stability (using

$Li_4Ti_5O_{12}$//$LiCoO_2$ full cells with a nominal voltage of ≈ 2.5 V). This is a study focused on filling the void existing in the literature and the need in the scientific and industrial communities regarding exhaustive characterizations of separator materials towards their use during the development of new materials for battery applications.

2. Experimental

Material

Non-woven macroporous battery separators provided by DreamWeaver (South Carolina, USA) were used for this study: DreamWeaver Gold (thickness: 25µm and 40µm) and DreamWeaver Silver (thickness: 25µm and 40 µm), hereinafter named DwGx and DwSx, respectively, where x is 25 or 40. These separators are made from a blend of microfibers, which provide scaffolding with high strength and a wide open structure, and nanofibers, which surround microfibers in a way that the average pore size is decreased and the pore size distribution is narrowed. As a consequence of this nano and microfibers distribution, resulting pores are non-oriented and, therefore, an isotropic behavior would be expected. Table 1 presents the most relevant properties regarding the investigated separators according to datasheets provided by the supplier.

Scanning electron microscopy (SEM)

The structural and morphological characterization of the films was performed using a FEI Teneo Scanning Electron Microscope (Thermo Fisher Scientific, The Netherlands).

Porosity measurements

The porosity and the pore diameter distribution were characterized using mercury intrusion porosimetry (AutoPore IV 9510, Micrometrics). Measurements were performed up to 414 MPa, the contact angle of Hg with the separators was assumed to be of 140° and the Hg surface tension equal to 480 dynes/cm. The samples weights ranged from 0.15 g to 0.19 g.

Thermal and thermomechanical characterization

The thermogravimetric analysis (TGA) of all separators was carried out by means of a Pyris TGA (Perkin Elmer, USA) thermogravimetric analyzer. Samples were heated in a platinum crucible from 30°C to 900°C at a heating rate of 10°C/min under nitrogen atmosphere. Onset temperature (T_{onset}) was calculated as the point of intersection between the tangent drawn at the point of greatest slope and the extrapolated base line.

Differential scanning calorimetry (DSC) studies were carried out to determine main thermal transitions, i.e. melting temperature. For this purpose, samples ~ 6 mg were heated up from -100°C to + 300°C (20°C/min) in closed aluminum capsules using a DSC822e (Mettler Toledo, Switzerland) under a 50 mL/min constant N_2 (g) flow.

Thermomechanical characterization was conducted on samples 3.5 mm x 4 mm using a DMA Q800 (TA Instruments, USA) working in tensile mode at 1 Hz and an oscillation amplitude of 15 µm. Measurements were carried out by triplicate in the temperature range from 30°C to 300°C during heating (5ºC/min).

Ionic conductivity measurements

Conductivity measurements were performed in an Impedance/Gain-Phase Analyzer SI1260 (Solartron, UK). Impedance tests were carried out by applying a 100 mV amplitude signal in the 1 Hz - 10 MHz frequency range. A solution 1M $LiPF_6$ in 1:1 ethylene carbonate and dimethyl carbonate (LP30, BASF) was used as reference electrolyte. Measurements at different temperatures, while heating from -30°C to +30°C, were carried out using stainless steel blocking electrodes (Φ=12 mm), dried overnight at 80°C under vacuum, which were embedded in a Swagelok-Teflon cell. Given their high trend to absorb humidity, before assembly, separators were dried in vacuum at 120ºC for 2 hours and later immersed in LP30 during 15 hours in argon atmosphere. The assembly of cells was performed in a glove box with argon atmosphere to

prevent moisture absorption. To obtain reproducible measurements, we established a dwell time of 30 minutes before taking every measurement, in order to reach a stable temperature.

Electrochemical characterization

Full cells bearing $LiCoO_2$ (LCO, >99.8%, Aldrich) as the positive electrode and Li_4Ti_5O12 (LTO, >99%, Aldrich) as the negative electrode were assembled. For experiments at slow discharge-charge rates, C/30 and C/10, composition of both negative and positive electrodes was 85% active material, 10% Super C65 (Timcal) conductive carbon and 5% PVDF (Kynarflex, Elf Atochem) binder. Here, electrodes were uniaxially pressed into pellets with an area of 0.5 cm^2 and dried at 80ºC overnight prior to assembly. On the other hand, for C-rate testing, both positive and negative electrodes were roll-pressed from slurries elaborated with NMP as solvent. In this case, composition of the negative electrode was 80% LTO, 10% Super C65 conductive carbon and 10% PVDF. Electrodes were punched into disks with an area of 1.13 cm^2 and dried at 80ºC for 24 hours under vacuum before use. The mass balancing of electrodes in full cells was done with a LCO:LTO ratio of capacities near 1 (or a LCO:LTO mass ratio near 1.28). The specific capacities are referred to the LCO positive electrode. Cell assembly was performed in a glove box with argon atmosphere (H_2O and O_2 content < 0.1 ppm) using the DreamWeaver Gold and Silver membranes (DwGx and DwSx, 25 and 40 μm) and the commercial PP macroporous membrane (Celgard® 2400, 33 μm) as separators. The electrolyte was 1M lithium hexafluorophosphate, $LiPF_6$, in EC:DMC 1:1 (LP30 Selectilyte, Merck, $H_2O \leq 20$ ppm).

Discharge and charge tests of full cells were performed in coin cells (CR2032 type, Hohsen) at 25ºC. The electrochemical galvanostatic experiments were controlled with a VMP3 multichannel galvanostat-potentiostat (Biologic). Cycling performance was tested at C/30 and C/10 constant current or at different current rate from C/10 to 2C in the 3.0 - 0.1 V voltage range, where “n” in “C/n” stands for the time needed (in hours) to insert/deinsert 1 Li+ per formula weight of compound, LCO.

3. Results and discussion

Despite there are several relevant applications in which high temperature operation is required, i.e. direct conversion-storage of photovoltaic energy (rooftop power station), most commercially available polyolefin-based separators are only used in the temperature range from –20°C to + 60°C [16]. Due to the increased demand for more reliable applications, polymer separators with higher thermal and electrochemical stability are required, activating the search for new materials capable of providing safer, more economical and reliable lithium-ion batteries.

3.1. Morphology and microstructural characterization

3.1.1. Scanning Electronic Microscopy (SEM)

Figure 1 shows a detailed view of the surface morphology, obtained by scanning electron microscopy (SEM) of DwG40 and DwS40 separators, a similar morphology was observed for those separators 25 μm thick. The manufacturing process used to produce these separators enables the attainment of a paper-like texture with a microstructure that combines microfibers and nanofibers. Microfibers provide an open support structure with high strength surrounded by nanofibers that allow obtaining not only a low average pore size but also a narrow pore size distribution, while still enabling ionic conductivity. The random distribution of both kinds of fibers suggests an isotropic behavior. The diameter of the microfibers is similar for all separators and close to 7 ± 1 μm, whereas the diameter of the nanofibers does not exceed 600 nm.

As seen in insets C and D of figure 1, small particles attached to the fibers were observed. Chemical analysis by means of Energy Dispersive Spectroscopy (EDS) (spot mode) revealed significant higher calcium content in such particles in comparison with the rest of the material. This calcium content might result from the dispersion process of para-aramid.

3.1.2. Mercury intrusion porosimetry

The macroporous character of the separators was investigated by mercury intrusion porosimetry. Figure 2 shows the cumulative pore volume and the pore size distribution through the derivate

distribution function (dV/dlogD) *vs* the pore diameter. The DwSx separators reach a similar total pore volume of about 1.5 $cm^3.g^{-1}$, which corresponds to a porosity of 69% for the DwS25 and 73% for the DwS40. For these separators, the cumulative pore volume curves present a similar trend, first a gradual increase of mercury intrusion, probably coming from the impregnation process, until a first step, centered at 5 µm and 9 µm for DwS25 and DwS40, respectively (Figure 2.b). Later on, the mercury intrusion continues increasing to reach a common plateau around 0.1 µm, describing thus the main window of the pore size distribution, which is centered around 1.7 µm for DwS25 and 2.3 µm for DwS40 (Figure 2.b). The presence of a step at 5 µm for the DwS25 and 9 µm for the DwS40 may be caused by the passage from the microfibers support to the network formed by the nanofibers, since the technique of mercury intrusion porosimetry considers the size of the entrance to a pore. Regarding the DwGx separators, it was not possible to make a clear distinction between them, probably because of the difference in affinity between mercury and substrate. For the DwGx separators the pore size distribution started around 9 µm and up to 0.1 µm, being centered at 3 µm for DwG25 and 1.7 µm for DwG40. The total pore volume reached 2.0 $cm^3.g^{-1}$ and 1.8 $cm^3.g^{-1}$ for DwG25 and DwG40, respectively, leading to a porosity of 78% and 67%, respectively. Both DwGx and DwSx separators exhibit larger porosity than alternative non-woven polyolefin membranes [10][11][17][18]. To summarize, the DwSx and DwGx separators are highly porous with a broad pore size distribution ranged from 9 to 0.1 µm, in accordance with SEM observations, without being possible to distinguish a clear trend according to their thickness neither their chemical nature.

3.2. Thermal and thermomechanical behavior

3.2.1. Thermogravimetric analysis (TGA)

Figure 3 presents the thermogravimetric analysis carried out on all separators under investigation. Unlike polyolefin separators, given their content of cellulose nanofibers, Dreamweaver separators present a high trend to retain moisture. Therefore, a first weight loss below 100°C is clearly observed for all of them. Water content was estimated as 4% and 2% for DwSx and DwGx,

respectively. This is in agreement with the supplier information, which recommends a drying process prior to usage, since silver and gold separators may contain some traces of moisture, up to 4% and 7%, respectively. At temperatures below 80ºC, no significant difference in behavior is noticed when comparing Dw separators with polyolefin-based ones. However, above such temperature, polyolefin-based separators usually start to experience shrinkage. This is a handicap regarding battery applications, since shrinkage could lead to the establishment of electrical contact between electrodes and, therefore, short-circuits.

On the other hand, thermal degradation of Dw separators, in the form of weight loss, starts at temperatures over 330°C, without melting. Onset temperatures were found to be about 331ºC for DwSx separators and 336ºC for DwGx ones, with only negligible differences (in the margin of error of the measurement instrument) according to the material thickness. As a result, it could be said that DwSx and DwGx separators present a higher thermal stability compared to those polyolefin-based separators, in which thermal degradation (under nitrogen) starts from roughly 290°C [16]. Moreover, DwGx separators presented slightly higher thermal stability compared to DwSx ones. This could be ascribed to their content of Twaron® para-aramid fibers, which enhances thermal, chemical and dimensional stability.

Despite the high capability to retain moisture, given their high thermal stability, drying processes can be successfully applied at relatively high temperatures (120-140°C) for short periods of time without producing any material degradation.

3.2.2. Differential scanning calorimetry (DSC)

DSC measurements were carried out for all separators. In all cases, two endothermic peaks can be clearly observed. Their maximum temperatures and associated enthalpies are summarized in table 2.

Given the high trend of these separators to absorb moisture, the first endothermic peak, located at temperatures around 100°C, is ascribed to water evaporation. Owing to their hydrophobic nature, such behavior is not commonly observed in polyolefin-based separators. Nevertheless, in

polyolefin-based separators as temperature increases and approaches about 80°C, they begin to shrink and then melt. Melting temperature for polypropylene (PP) and polyethylene (PE) based separators are about 165°C and 140°C, respectively [16]. This is an asset regarding safety, since when pores collapse, shutting down of the cell occurs, preventing thermal runaway reactions to take place. However, if shrinkage becomes excessive, electrical contact between electrodes can be established, and, therefore, a short circuit can occur. Despite Dw separators do not have a shutdown function at relatively low temperatures as polyolefin-based ones, they do not melt or shrink during a battery normal operation, reducing occurrence of short-circuits and, therefore, improving safety. The second endothermic peak, which takes place at about 250°C, could be associated to the melting of polyethylene terephthalate (PET), the thermoplastic component that enables cells shutting down.

3.2.3. Thermomechanical behavior

Dw separators present high porosity with a relatively broad pore size distribution. In addition, their chemical composition based in aramid fibers provides them not only with high thermal stability, as seen after TGA and DSC measurements, but also with good chemical resistance and mechanical strength. To investigate mechanical properties of the separators, they were tested by DMTA both, in machine and transverse direction (MD and TD, respectively). Figure 4 (left) shows the storage modulus (E') as a function of temperature for the whole temperature range tested (30°C - 300°C).

Table 3 summarizes modulus of elasticity (E'), at room temperature and 70°C, and tan δ, whose maximum can be related with transition α so, roughly, with glass transition temperature (T_g).

For all cases, an increase in elastic modulus is observed when compared with polyolefin-based separators, whose maxima E' reach values ranging from 200 to 400 MPa at 70°C, unlike Dw, which present E' values up to 1.5 GPa (DwS25) at the same temperature. Such a large difference in E' is reflected in the shrinkage usually observed by both kinds of separators. Polyolefin-based separators usually start shrinkage when the temperature approaches 75°C and reach catastrophic

levels at 100°C [16]. On the other hand, DwSx and DwGx separators, given their structural configuration and backbone material, present a negligible shrinkage, < 0.5% up to 250°C (see figure 5).

When comparing DwGx separators (different thicknesses), only negligible differences were observed regarding E'. Nevertheless, in case of DWSx, a higher modulus of elasticity was observed for those samples 25 μm thick. This could be associated to the porosity percentage, which is larger in case of those separators 40 μm thick (see table 1). Moreover and despite of their improved porosity, E' values of Dw separators are significantly larger than alternative membranes [10][18]; we consider that micro- and nanofibrous morphology plays a key role in the physical properties of Dw separators, in contrast to woven- and non-woven-based alternatives.

Regarding MD and TD, slight differences in E' were observed for all separators, suggesting a nearly isotropic behavior, which is in accordance with previous results obtained for tensile strength by Kalnaus et. al. [14]. Concerning glass transition temperature (indeed transition α), measured as the maximum of tan δ in figure 4 (right), no significant differences were observed when measurements were performed in TD and MD.

3.2.4. Electrochemical characterization

a) Ionic conductivity

As a proof of concept and to assess their potential as alternative separators, conductivity was measured by drying separators at 120ºC under vacuum for 2 hours and soaking them in benchmark LP30 electrolyte for 15 hours; all procedures were performed in a glove box in argon atmosphere. Figure 6 shows conductivity measurements obtained at different temperatures (-30°C to +30°C) during heating. As temperature increases, conductivity also does, until a nearly plateau response is obtained from 10ºC on. Maximum ionic conductivity was obtained for DwG40, which allowed reaching a maximum value of 6.2×10^{-4} $S.cm^{-1}$ at 12.5ºC. Values obtained are lower than those reached by commercial polyolefin-based separators, in the range of 10^{-3} $S.cm^{-1}$ at 30ºC. The conductivity loss, with regard to polyolefin separators, cannot be ascribed (i) to a lesser open

porosity, as porosities determined by mercury porosimetry approach or exceed 70% or (ii) to a poor wettability of pores by the liquid electrolyte, as DwG and DwS have good interactions with this polar electrolyte. This has been indirectly demonstrated by the failure of the contact angle measurement: indeed water and LP30 drops are absorbed in just a few seconds after surface contact with DreamWeavers separators. Therefore, both the porosity level and the interaction quality should lead to higher conductivities for the set DwG/LP30 than for the set Celgard/LP30. We will discuss this surprising result vide infra (3.3.Discussion).

We must however mention that higher ionic conductivities, namely 1.56 mS cm^{-1} and 1.16 mS cm^{-1}, have been reported at 25°C for DwG20 and DwS25, respectively, using sodium perchlorate based carbonates electrolytes ($NaClO_4$, 1M in EC : DMC 1:1 by volume) [19].

Table 4 presents the MacMullin number (N_M) and tortuosity τ calculated from Eqs. (1) and (2) [20]:

$$N_M = \sigma_0/\sigma_{eff} \quad (1)$$

$$\tau = (N_M \times \varepsilon)^{1/2} \quad (2)$$

where σ_0 and σ_{eff} are the conductivities of the liquid electrolyte (LP30®) and those of the set separator + liquid electrolyte, respectively, and ε is the porosity.

The MacMullin number characterizes the effect of the macroporous separator on the ionic conductivity of the liquid electrolyte (LP30®). N_M is inversely proportional to the effective transport coefficient (δ_{eff}), which is influenced by the porous structure of the separator and its molecular interactions with the liquid electrolyte. The estimated N_M for these systems are comparable to those of some polyolefin based separators (Celgard®2325 and aged Celgard®2325-2400). In addition, their high porosity contributes to obtain a higher tortuosity, which is coherent with their labyrinth-like pore structure and has been already reported for other kind of non-woven separators [21], although it is not the common trend for such structure. Indeed, high porosity is generally associated to a low tortuosity for non-woven separators. Hence, the obtained results are probably related to the low conductivity values obtained.

b) Electrochemical tests on LTO//LCO cells

The electrochemical performance of the full cell $Li_4Ti_5O_{12}/LiCoO_2$ (LTO/LCO) using non-woven macroporous Dw separators was studied by means of cycling tests performed at different charge-discharge rates. The charge rates used were from C/30 (30 h) to 2C (30 min). The voltage profile versus capacity at C/30 rate is shown for a LTO/LP30®+DwGx/LCO and LTO/LP30®+DwSx/LCO cell in Figure 7a and 7b, respectively. For such low charge rate, the electrochemical performance of the different cells is very similar; the charge-discharge capacities being 137 mAh g^{-1} developed at ca. 2.45 V in the lithium-ion cells regardless the separator used. To investigate the charge-discharge cycling performance, the LTO/LP30®+DwGx/LCO and LTO/LP30®+DwSx/LCO cells were tested at a C/10 rate. Figure 8 shows the first charges for both DwSx (Fig. 8a) and DwGx (Fig. 8b) separators having thicknesses of 25 and 40 μm at C/10, as well as the reversible specific capacity and efficiency (Fig. 8c and Fig 8d) for the first 10 cycles. Initial capacities of lithium-ion cells using DwG25, DwG40, DwS25 and DwS40 are very similar and close to the theoretical capacity (137 mAh g^{-1}), which demonstrates similar behavior upon cycling regardless the type and thickness of the separator used in the battery. After 10 cycles, the capacities became 136.9, 135.2, 136.9 and 136.9 mAh g^{-1}, leading to capacity retention rates of 100%, 98.8%, 100% and 100%, for DwG25, DwG40, DwS25 and DwS40, respectively. All separators exhibit excellent and stable Coulombic efficiency and no significant differences can be found in terms of thickness and separator type employed at this particular C rate.

The electrochemical performance of cells was further investigated by evaluating the charge-discharge capability at different C rates from C/10 (0.073 mA cm^{-2}) to 2 C (1.46 mA cm^{-2}). Figure 9 compares the result of these tests with DwG25 (blue circle), DwG40 (red square), DwS25 (green triangle) and DwS40 (pink diamond) separators. To better compare the separators, the charging capacities were normalized using those obtained at a low charge rate, C/10. Results are presented as a function of charge rate in Fig. 10. As with the lowest C/30 rate, for relatively low charge rates C/10, C/5 and C/3, the electrochemical performance of the different cells is similar, the capacities

being ~137 mAh g^{-1}. From these data it can be inferred that the separator type has no significant effect on the battery performances. Li^+ ion mobility in the electrolyte (liquid + separator as a whole), therefore does not play a limiting role under these experimental conditions. On the contrary, the charge capacity developed at higher C rates, C/2, 1C and 2C, considerably depends on the separator used. In contrast to low C rates, the transport processes in the electrolyte seems to become the limiting process at these higher C rates, while they were seen not to be critical at lower C rates. This indicates a dependence of the electrochemical performance of the battery on the porous structure of the separator, in connection with ion conductivity and ion concentration gradient in both the bulk electrolyte and inside the electrode [20]. It is noteworthy to mention that the best performance at high charge rates was obtained in batteries using DwG40 as separator. The DwG40 separator shows the highest porosity, highest ionic conductivity (σ), highest effective conductivity (σ_{eff}), lowest MacMullin number (N_M) and tortuosity (τ) of all separators. The severe capacity loss at 2C observed in DwG25, DwS25 and DwS40 may be due to the structure of the separator, i.e. porosity, thickness and pore structure, which decreases ionic mobility.

3.3. Discussion

Fairly neglected by academic researchers as emphasized by Arora et al.[22], macroporous or dense separators are however essential and should be improved in terms of safety (thermomechanical stability) of performances and of cost saving.

These separators exhibit indisputable advantages *vs* commercial polyolefins-based separators as Solupor® and Celgard® in terms of thermomechanical stability and, especially, their absence of shrinkage. Hence, it can be expected a good performance for batteries operating at higher temperatures than the current Li-ion batteries. Their liquid electrolyte filling is faster than in the case of the polypropylene and the 3-layered polypropylene/polyethylene/polypropylene separators, Celgard®2400 and Celgard®2325, respectively, as demonstrated while trying to measure contact angle (wettability). Table 5 compares conductivity obtained for the sets polyolefin separator/LP30 and DwS or DwG/LP30 at 21°C.

The first line of conductivities are extracted from Djian *et al.* [20], the second one from Martinez-Cisneros *et al.*[16]. The gap, sometimes very important, is due to the low kinetics of filling processes of non-polar separators with a polar liquid electrolyte. Thus, Martinez *et al.*[16] increased the impregnation time from 1 hour to 12 hours. Even though Dw sets are compared to the lowest conductivities of the *state of the art*, they are inferior. This can neither be ascribed to the filling kinetics, as Dw separators are much more polar than the usual polyolefin-based separators, nor to an insufficient open porosity, as their porosity exceeds the Celgard ones and are close to the Solupor ones.

Unexpected conductivity losses could be ascribed to the increased polarity of Dw separators compared to polyolefin ones. Indeed Nylon-type aliphatic polyamides have a very high affinity for the lithium salts that can lead, besides, to the mechanical degradation up to the dissolution of woven fabrics [23]. If amide groups are present in DwG separators, they belong to highly crystalline polyaramid fibres, which are insensitive to this mechanical degradation. Due to the acidity of the -CONH moiety, DwG separators are endowed with high Acceptor Number (AN) prone to strongly interact with the PF_6^- anion. Moreover, the carbonyl should interact with the Li^+ cation (DN, Donor Number); both interactions decreasing ion's mobility, thus the ionic conductivity. Regarding DwS separators, they are based on polyacrylonitrile, whose 'pseudo-acidic' hydrogen (*in α position of the nitrile group*) can interact with PF_6^- and whose nitrile groups are known to have high affinity towards Li^+. Thus, a slowdown of both anion and cation diffusion can explain the conductivity decrease. Beyond the performance of commercial macroporous separators, it should be emphasized that non-commercial ones, based on PVdF homopolymers, have significantly lower NM, which ranges between 2.45 and 3.6. This depends on the liquid electrolyte [24]. Despite the affinity of PVdF for the liquid electrolytes solvents - EC, PC, DMC, EMC – favors the pore wettability as well as the retention of liquid electrolytes, it decreases its thermomechanical stability [24].

Regarding the electrochemical performance of Dw separators, they exhibit, at low C rates, similar characteristics than Celgard®2400 operated under the same cycling conditions [28][29].

Nonetheless, the tests performed at higher C rates tnah C/3 allow discriminating between the Dreamweaver separators. Among Dw separators, the best performances, up to 1C, were obtained with the most conductive sets i.e. DwG40/LP30 followed by DwS40/LP30. At higher C rate, 2C, DwG40/LP30 provided high cyclability as compared to the poor cycling performances of both the other Dw separators and Celgard®2400. The gap between DwG40 and Celgard®2400 is all the more surprising as Celgard thickness is roughly half DwG40 one.

4. Conclusions

The thorough investigation of the polyaramid-based separators leads to mixed results. Among the main advantages of the best Dw separators, it can be quoted (i) the rapid filling of their open porosity; an unquestionable processing asset and (ii) the absence of shrinkage allowing high temperature operation. Regarding the electrical and electrochemical properties, balance of both characteristics is positive to Dw separators. Although conductivity values of separators are somewhat modest, the electrochemical performance developed when used in a $Li_4Ti_5O_{12}/LiCoO_2$ cells are, at moderate C ates, comparable to commercial Celgard©2400 separator. At high C rates, in particular at 2C, DwG40 exhibits much higher capacities than the whole of the separators, including Celgard®2400. A further contribution comparing the cycling behavior at different temperatures of both DwG and DwS with state of art separators is currently in progress towards providing the scientific and industrial community with a thorough ranking that enables selecting the best approach for the evaluation of new materials for electrolytes and electrodes.

5. Acknowledgements

We thank “Agencia Estatal de Investigación/Fondo Europeo de Desarrollo Regional” (FEDER/UE) for funding the projects MAT2016-78362-C4-3-R, MAT2016-78362-C4-1-R, PID2019-106662RB-C41 and PID2019-106662RB-C44. The regional government of

Comunidad de Madrid is acknowledged for funding the project MATERYENER3CM S2013/MIT-2753.

J-Y Sanchez acknowledges the CONEX Programme, funding received from Universidad Carlos III de Madrid, the European Union's Seventh Framework Programme for research, technological development and demonstration (Grant agreement nº 600371), Spanish Ministry of Economy and Competitiveness (COFUND2013-40258) and Banco Santander.

The authors would like to acknowledge DreamWeaver for samples supply.

6. References

[1] M.F. Lagadec, R. Zahn, V. Wood, Characterization and performance evaluation of lithium-ion battery separators, Nat. Energy. 4 (2019) 16–25. https://doi.org/10.1038/s41560-018-0295-9.

[2] X. Huang, Separator technologies for lithium-ion batteries, J. Solid State Electrochem. 15 (2011) 649–662. https://doi.org/10.1007/s10008-010-1264-9.

[3] E. Foreman, W. Zakri, M. Hossein Sanatimoghaddam, A. Modjtahedi, S. Pathak, A.G. Kashkooli, N.G. Garafolo, S. Farhad, A Review of Inactive Materials and Components of Flexible Lithium-Ion Batteries, Adv. Sustain. Syst. 1 (2017) 1700061. https://doi.org/10.1002/adsu.201700061.

[4] V. Deimede, C. Elmasides, Separators for Lithium-Ion Batteries: A Review on the Production Processes and Recent Developments, Energy Technol. 3 (2015) 453–468. https://doi.org/10.1002/ente.201402215.

[5] S.S. Zhang, A review on the separators of liquid electrolyte Li-ion batteries, J. Power Sources. 164 (2007) 351–364. https://doi.org/10.1016/j.jpowsour.2006.10.065.

[6] H. Lee, M. Yanilmaz, O. Toprakci, K. Fu, X. Zhang, A review of recent developments in membrane separators for rechargeable lithium-ion batteries, Energy Environ. Sci. 7 (2014) 3857–3886. https://doi.org/10.1039/c4ee01432d.

[7] E. Wang, H.-P. Wu, C.-H. Chiu, P.-H. Chou, The Effect of Battery Separator Properties

on Thermal Ramp, Overcharge and Short Circuiting of Rechargeable Li-Ion Batteries, J. Electrochem. Soc. 166 (2019) A125–A131. https://doi.org/10.1149/2.0381902jes.

[8] X. Feng, M. Ouyang, X. Liu, L. Lu, Y. Xia, X. He, Thermal runaway mechanism of lithium ion battery for electric vehicles: A review, Energy Storage Mater. 10 (2018) 246–267. https://doi.org/10.1016/j.ensm.2017.05.013.

[9] S. Ma, H. Lin, L. Yang, Q. Tong, F. Pan, J. Weng, S. Zheng, High thermal stability and low impedance polypropylene separator coated with aluminum phosphate, Electrochim. Acta. 320 (2019). https://doi.org/10.1016/j.electacta.2019.07.039.

[10] C.M. Costa, M. Kundu, J.C. Dias, J. Nunes-Pereira, G. Botelho, M.M. Silva, S. Lanceros-Méndez, Mesoporous poly(vinylidene fluoride-co-trifluoroethylene) membranes for lithium-ion battery separators, Electrochim. Acta. 301 (2019) 97–106. https://doi.org/10.1016/j.electacta.2019.01.178.

[11] N. Wei, J. Hu, M. Zhang, J. He, P. Ni, Cross-linked porous polymer separator using vinyl-modified aluminum oxide nanoparticles as cross-linker for lithium-ion batteries, Electrochim. Acta. 307 (2019) 495–502. https://doi.org/10.1016/j.electacta.2019.04.010.

[12] B. Morin, J. Hennessy, P. Arora, Developments in nonwovens as specialist membranes in batteries and supercapacitors, in: Adv. Tech. Nonwovens, Elsevier Inc., 2016: pp. 311–337. https://doi.org/10.1016/B978-0-08-100575-0.00011-5.

[13] B. Morin, C. Hu, P. Khokhlov, J. Kaschmitter, S.-J. Cho, Safety Testing with Nonwoven Nanofiber Separators: Comparing Shutdown Separators to Thermally Stable Separators, ECS Trans. 72 (2016) 1–12. https://doi.org/10.1149/07212.0001ecst.

[14] S. Kalnaus, Y. Wang, J.A. Turner, Mechanical behavior and failure mechanisms of Li-ion battery separators, J. Power Sources. 348 (2017) 255–263. https://doi.org/10.1016/j.jpowsour.2017.03.003.

[15] G.M. Veith, B.L. Armstrong, H. Wang, S. Kalnaus, W.E. Tenhaeff, M.L. Patterson, Shear Thickening Electrolytes for High Impact Resistant Batteries, ACS Energy Lett. 2 (2017) 2084–2088. https://doi.org/10.1021/acsenergylett.7b00511.

[16] C. Martinez-Cisneros, C. Antonelli, B. Levenfeld, A. Varez, J.Y. Sanchez, Evaluation of polyolefin-based macroporous separators for high temperature Li-ion batteries, Electrochim. Acta. 216 (2016) 68–78. https://doi.org/10.1016/j.electacta.2016.08.105.

[17] D. Karabelli, J.C. Leprêtre, F. Alloin, J.Y. Sanchez, Poly(vinylidene fluoride)-based macroporous separators for supercapacitors, in: Electrochim. Acta, Elsevier Ltd, 2011: pp. 98–103. https://doi.org/10.1016/j.electacta.2011.03.033.

[18] J. Hu, Y. Liu, M. Zhang, J. He, P. Ni, A separator based on cross-linked nano-SiO2 and cellulose acetate for lithium-ion batteries, Electrochim. Acta. 334 (2020). https://doi.org/10.1016/j.electacta.2019.135585.

[19] N.I. Globa, Y. V. Shmatok, O.I. Milovanova, V.A. Sirosh, S.A. Kirillov, Electrolytic Double-Layer Supercapacitors Based on Sodium-Ion Systems, with Activated-Carbon Electrodes, Russ. J. Appl. Chem. 91 (2018) 187–195. https://doi.org/10.1134/S1070427218020039.

[20] D. Djian, F. Alloin, S. Martinet, H. Lignier, J.Y. Sanchez, Lithium-ion batteries with high charge rate capacity: Influence of the porous separator, J. Power Sources. 172 (2007) 416–421. https://doi.org/10.1016/j.jpowsour.2007.07.018.

[21] W. Yi, Z. Huaiyu, H. Jian, L. Yun, Z. Shushu, Wet-laid non-woven fabric for separator of lithium-ion battery, J. Power Sources. 189 (2009) 616–619. https://doi.org/10.1016/j.jpowsour.2008.09.078.

[22] P. Arora, Z. Zhang, Battery separators, Chem. Rev. 104 (2004) 4419–4462. https://doi.org/10.1021/cr020738u.

[23] D. Karabelli, J.C. Leprêtre, L. Cointeaux, J.Y. Sanchez, Preparation and characterization of poly(vinylidene fluoride) based composite electrolytes for electrochemical devices, Electrochim. Acta. 109 (2013) 741–749. https://doi.org/10.1016/j.electacta.2013.07.145.

[24] J. Saunier, F. Alloin, J.Y. Sanchez, G. Caillon, Thin and flexible lithium-ion batteries: Investigation of polymer electrolytes, in: J. Power Sources, 2003: pp. 454–459. https://doi.org/10.1016/S0378-7753(03)00197-6.

[25] C. Arbizzani, F. Colò, F. De Giorgio, M. Guidotti, M. Mastragostino, F. Alloin, M. Bolloli, Y. Molméret, J.Y. Sanchez, A non-conventional fluorinated separator in high-voltage graphite/LiNi 0.4Mn1.6O4 cells, J. Power Sources. 246 (2014) 299–304. https://doi.org/10.1016/j.jpowsour.2013.07.095.

[26] J.C. Barbosa, J.P. Dias, S. Lanceros-Méndez, C.M. Costa, Recent advances in poly(Vinylidene fluoride) and its copolymers for lithium-ion battery separators, Membranes (Basel). 8 (2018). https://doi.org/10.3390/membranes8030045.

[27] J.-P. Belières, M. Marechal, J. Saunier, F. Alloin, J.-Y. Sanchez, Swollen Polymethacrylonitrile Urethane Networks for Lithium Batteries, J. Electrochem. Soc. 150 (2003) A14. https://doi.org/10.1149/1.1521755.

[28] J.H. Kim, S.Y. Bae, J.H. Min, S.W. Song, D.W. Kim, Study on the cycling performance of Li 4Ti 5O 12/LiCoO 2 cells assembled with ionic liquid electrolytes containing an additive, Electrochim. Acta. 78 (2012) 11–16. https://doi.org/10.1016/j.electacta.2012.05.161.

[29] A. Wei, J. Mu, R. He, X. Bai, Z. Liu, L. Zhang, Z. Liu, Y. Wang, Preparation of Li4Ti5O12/carbon nanotubes composites and LiCoO2/Li4Ti5O12 full-cell with enhanced electrochemical performance for high-power lithium-ion batteries, J. Phys. Chem. Solids. 138 (2020). https://doi.org/10.1016/j.jpcs.2019.109303.

FIGURES

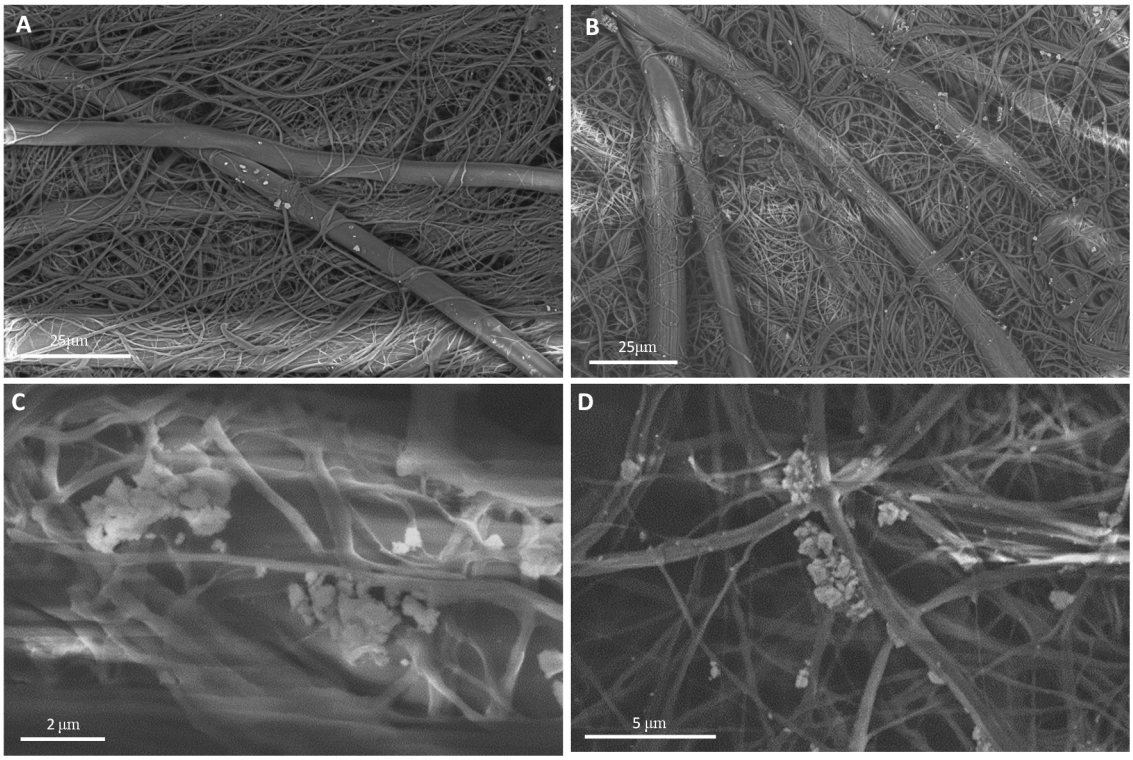

Figure 1. SEM images of pristine materials. A: DwS40 (Silver 40 µm thick). B: DwG40 (Gold 40 µm thick). C: zoom in of DwS40; D: zoom in of DwG40.

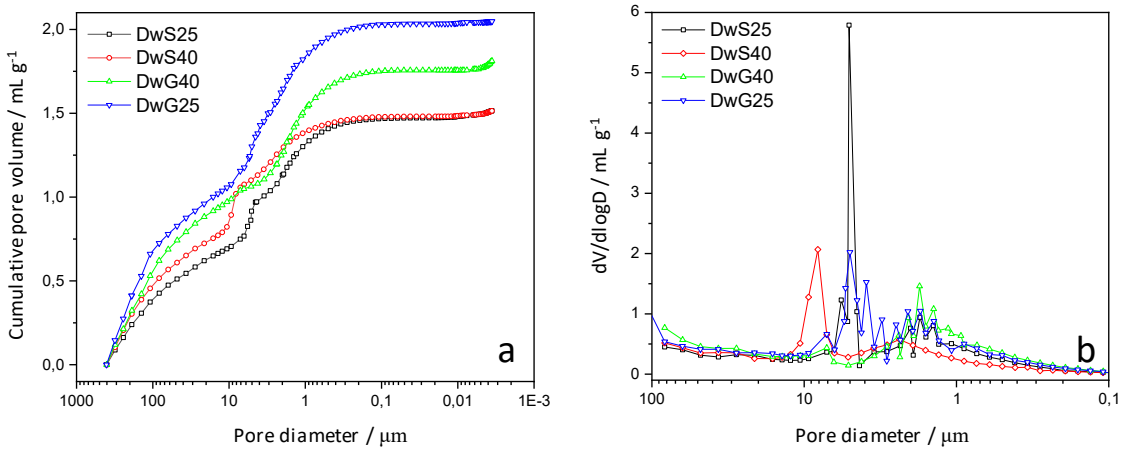

Figure 2. a) Cumulative pore volumes and b) macropore size distributions obtained from mercury intrusion porosimetry for the different separators.

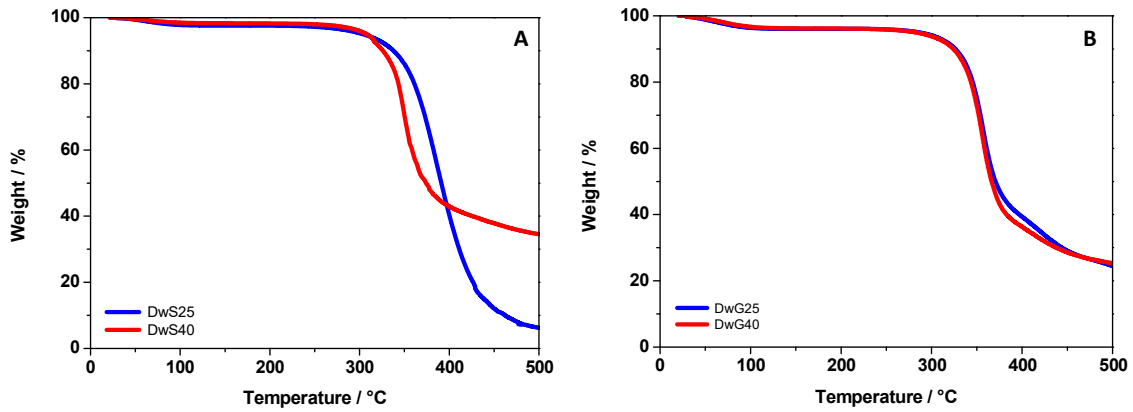

Figure 3. Thermogravimetric analysis of all separators: silver-based separators (A) and gold-based separators (B).

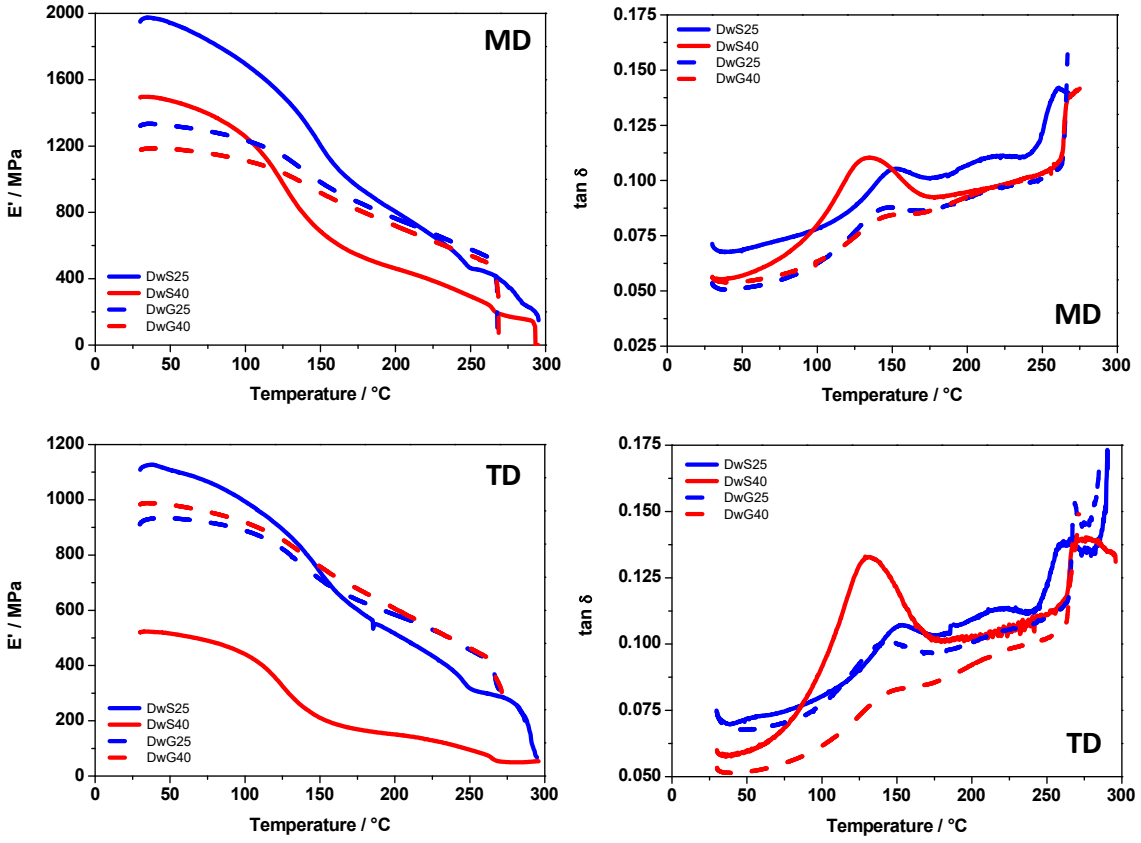

Figure 4. Modulus of elasticity (E') and tan δ for all separators evaluated in machine direction (MD) and transverse direction (TD).

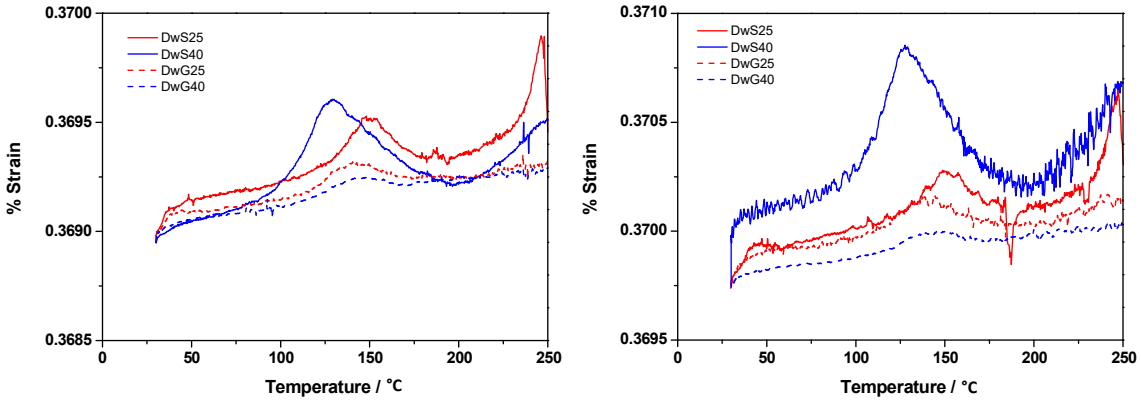

Figure 5. DMTA analysis reflecting cumulative strain presented by all four separators when evaluated in a wide temperature range; left: machine direction (MD); right: transverse direction (TD).

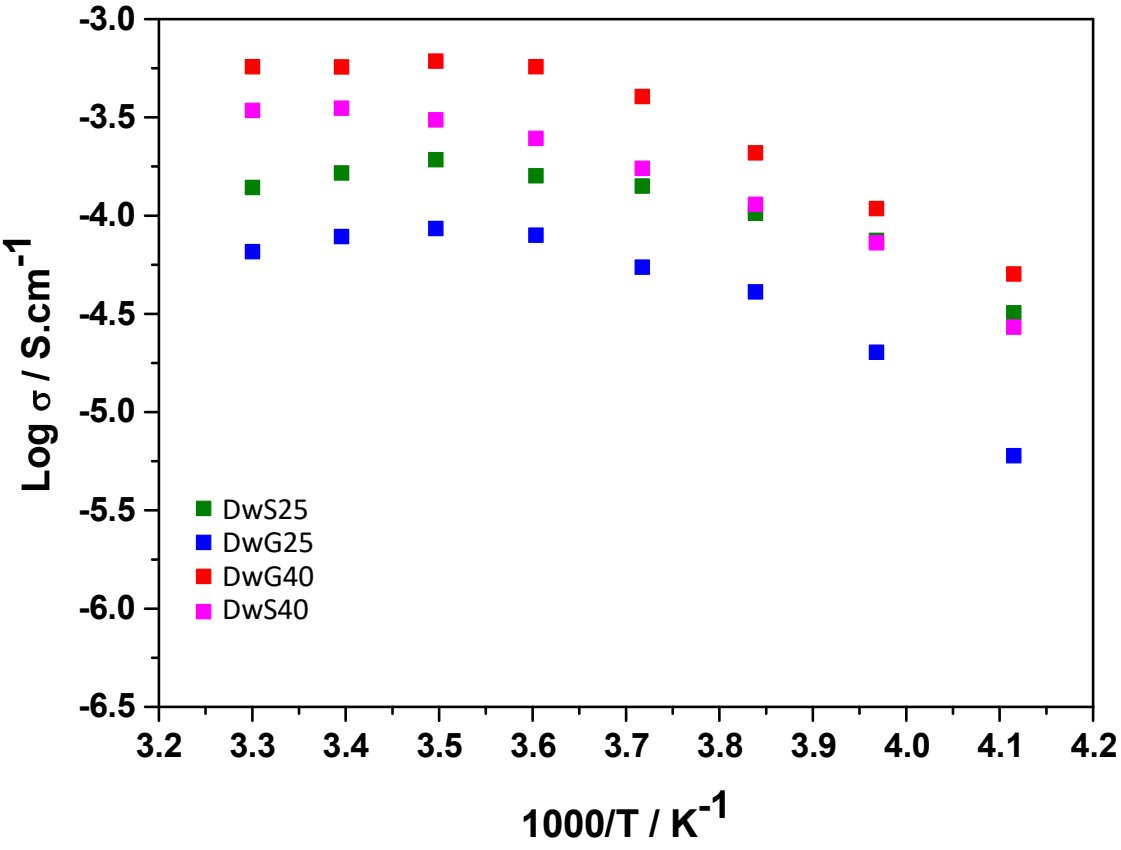

Figure 6. Conductivity measurements using LP30 as liquid electrolyte.

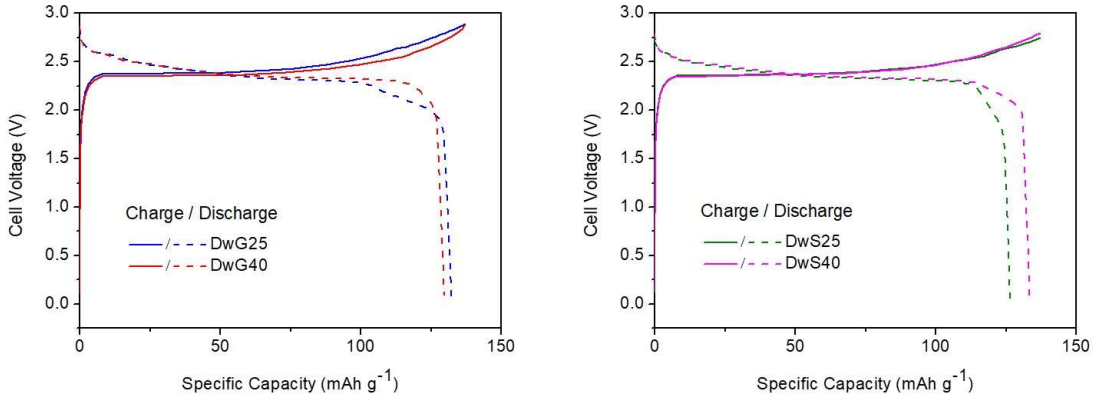

Figure 7. Charge / discharge (continuous / discontinuous line) first electrochemical profile for a) DwGx and b) DwSx (being x = 25 and 40 μm thicknesses) at C/30.

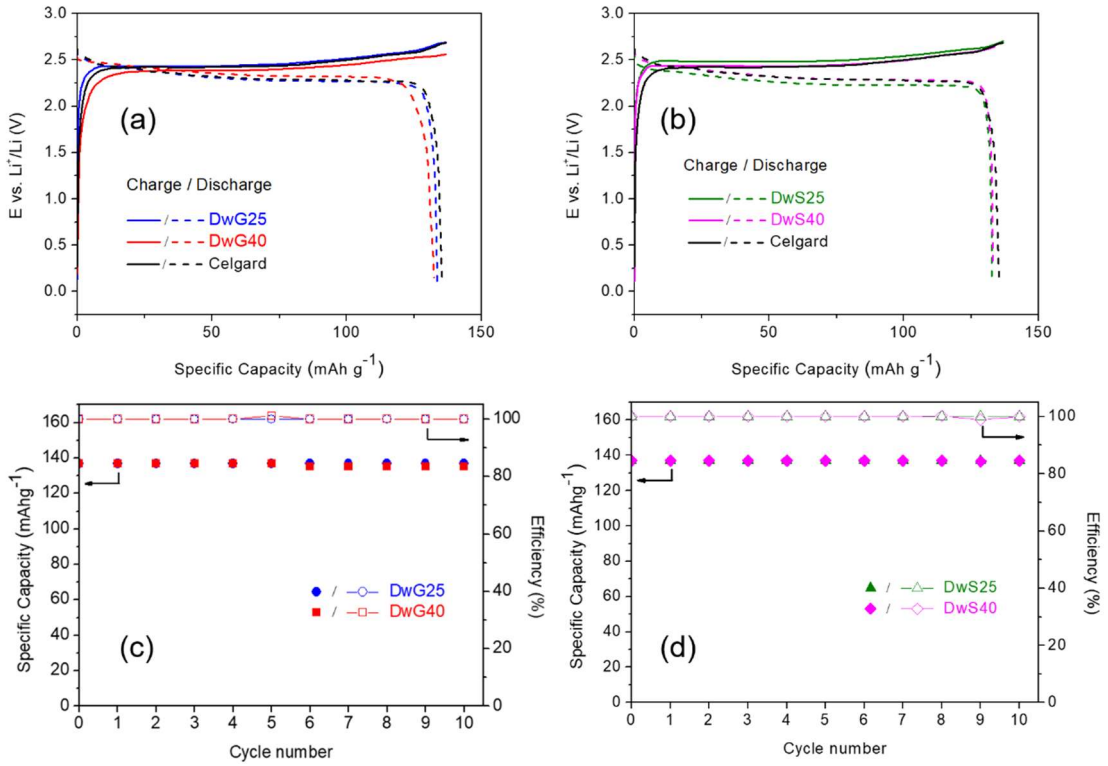

Figure 8. Comparison of electrochemical charge and discharge of cells with DwG25, DwG40 (a) and DwS25, DwS40 (b) separators. For comparison, Celgard©2400 is included. (c) and (d) Reversible capacities (full symbols) and efficiencies (empty symbols) for DwG and DwS separators, respectively.

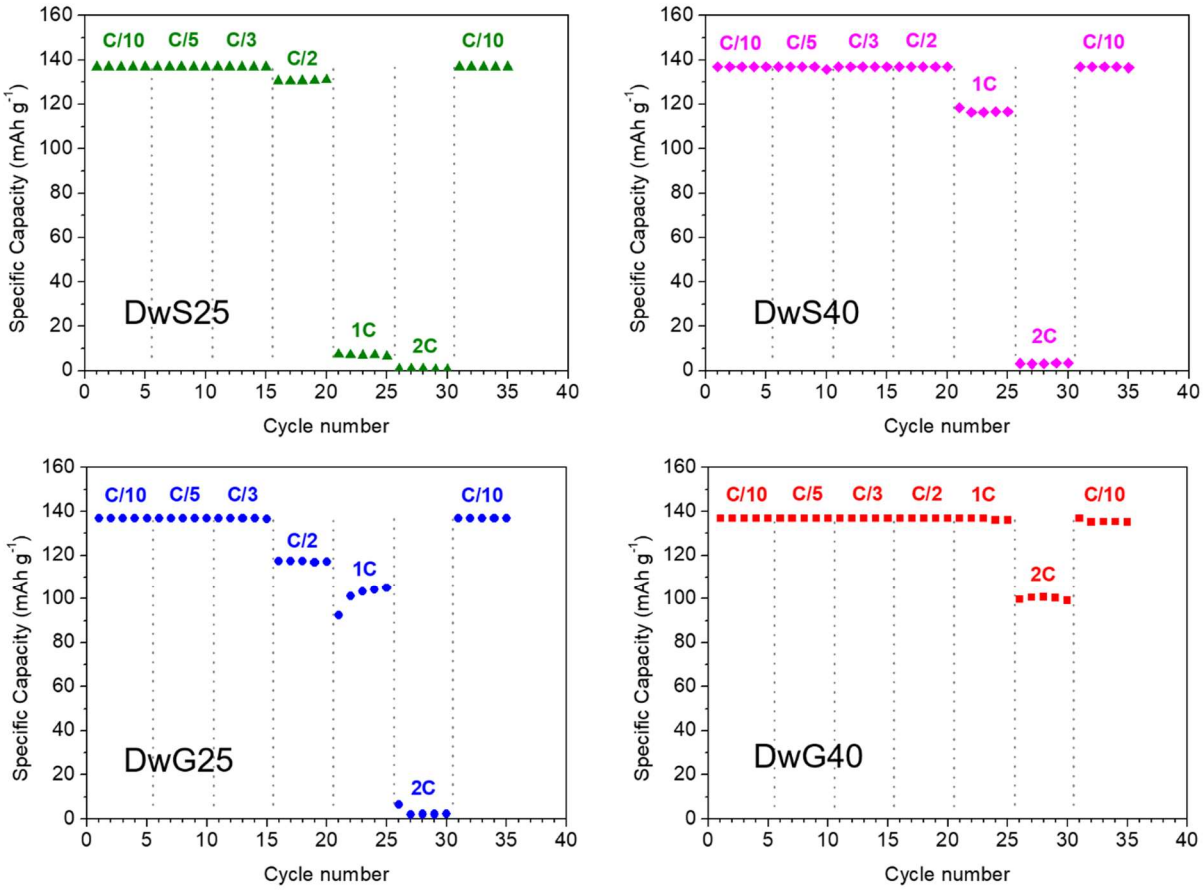

Figure 9: Comparison of the rate capability of $Li_4Ti_5O_{12}/LiCoO_2$ cells with non-woven macroporous Dw separators in the 0.1-3.0 V voltage range.

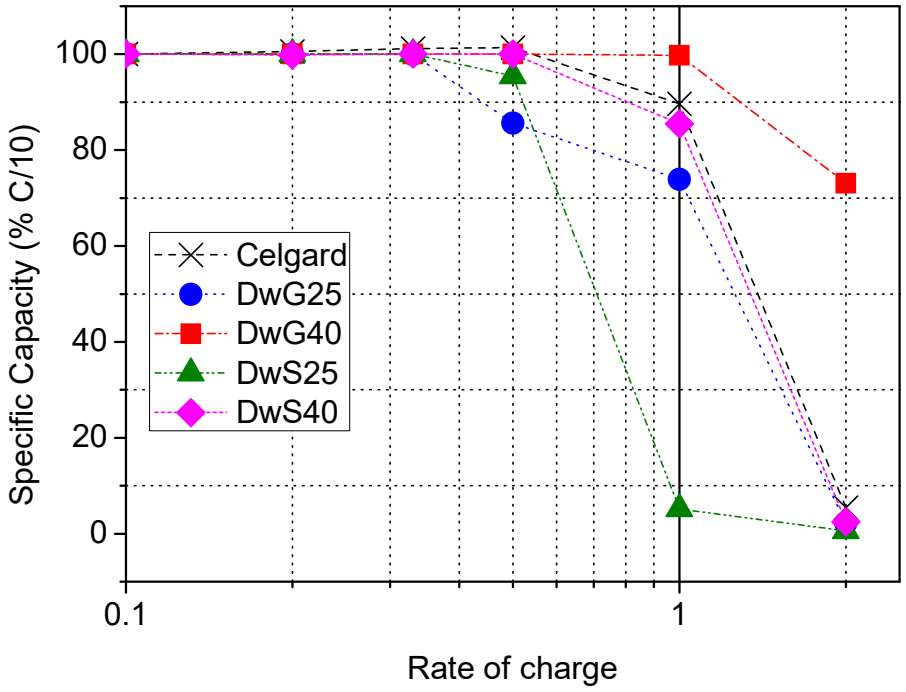

Figure 10: Normalized capacities for different charge rates

TABLES

Table 1. Main properties of DwGx and DwSx separators according to the supplier.

	DwGx		**DwSx**	
Thickness (x, μm)	25	40	25	40
Porosity (%)	61	68	56	60
Pore size diameter (μm)	0.6	0.6	1.1	0.4
Tensile strength, MD (Kgf/cm^2)	190	140	330	225
Tensile strength, TD (Kgf/cm^2)	80	75	175	105
Young's Modulus (Kgf/cm^2)	12000	15000	23000	14000
Melt integrity (ºC)	300	300	300	300

MD: machine direction; TD: transverse direction

Table 2. Melting and degradation temperatures (T1 and T2) and enthalpy of fusion obtained for all separators by DSC measurements.

Separator	**DwS25**	**DwS40**	**DwG25**	**DwG40**
T_1 (ºC)	105.5	82.7	96.6	110.0
ΔH_2 (J/g)	122.4	69.3	112.2	129.6
T_2 (ºC)	243.1	253.6	253.7	254.2
ΔH_2 (J/g)	35.8	13.0	12.4	10.3

Table 3. Modulus of elasticity (E') and glass transition temperature 1 (Tg), obtained as the maximum of tan δ, for all four separators in machine (MD) and transverse direction (TD).

Separator	E' (MPa)				T_g (ºC)	
	TD		MD		TD	MD
	30ºC	70ºC	30ºC	70ºC	ºC	ºC
DwS25	1110	1080	1950	1860	153	153
DwS40	520	500	1490	1420	132	133
DwG25	930	920	1320	1300	146	150
DwG40	980	960	1180	1160	154	154

Table 4. Effective conductivity (σ_{eff}) MacMullin number (N_M) and tortuosity (τ) of the set "LP30®+Dreamweaver separators" at 21ºC with $\sigma_0 = 9.8 \cdot 10^{-3}$ S·cm^{-1}.

Porous separator	σ_{eff} (mS·cm^{-1})	N_M	ε %*	τ	ε %**	T
DwS25	0.165	59.5	56	5.8	69	6.4
DwS40	0.331	29.6	60	8.3	73	9.2
DwG25	0.078	125.5	61	8.7	78	9.9
DwG40	0.715	13.7	68	3.0	67	3.0

* data from supplier
** data obtained from Hg porosimetry

Table 5. Conductivity achieved at 21ºC using LP30 as liquid electrolyte (units: mS·cm^{-1})

Celgard® 2400	Celgard® 2325	Solupor® 10P05A	Solupor® 3P07A	DwS25	DwS40	DwG25	DwG40
0.6	-	2.1	0.7	-	-	-	-
1.7	0.7	1.7	2.7	0.17	0.33	0.08	0.72